Toward more realistic social distancing policies via advanced feedback control

Cédric Join, Alberto D'onofrio, Michel Fliess

Toward More Realistic Social Distancing Policies via Advanced Feedback Control

Cédric Join [1,4,†] ![ORCID], **Alberto d'Onofrio** [2,†] ![ORCID] and **Michel Fliess** [3,4,*,†] ![ORCID]

1   CRAN (CNRS, UMR 7039), Université de Lorraine, BP 239, 54506 Vandœuvre-lès-Nancy, France; cedric.join@univ-lorraine.fr
2   Dipartimento di Matematica e Geoscienze, Università di Trieste, Via Alfonso Valerio 12, 34127 Trieste, Italy; alberto.donofrio@units.it
3   LIX (CNRS, UMR 7161), École polytechnique, 91128 Palaiseau, France
4   A.L.I.E.N., 7 rue Maurice Barrès, 54330 Vézelise, France; cedric.join@alien-sas.com (C.J.); michel.fliess@alien-sas.com (M.F.)
*   Correspondence: michel.fliess@polytechnique.edu
†   These authors contributed equally to this work.

Abstract: A continuously time-varying transmission rate is suggested by many control-theoretic investigations on non-pharmaceutical interventions for mitigating the COVID-19 pandemic. However, such a continuously varying rate is impossible to implement in any human society. Here, we significantly extend a preliminary work (M. Fliess, C. Join, A. d'Onofrio, Feedback control of social distancing for COVID-19 via elementary formulae, MATHMOD, Vienna, 2022), based on the combination of flatness-based and model-free controls with respect to the classic parsimonious SIR model. Indeed, to take into account severe uncertainties and perturbations, we propose a feedback control where the transmission rate, i.e., the control variable, is piecewise constant. More precisely, the transmission rate remains constant during an appreciable time interval, which is not too large. Strict extended lockdowns may therefore be avoided. The poor knowledge of fundamental quantities such as the rate of infection hinders a precise calibration of the transmission rate. Thus, the results of our approach ought therefore not to be regarded as rules of action to follow accurately but as a guideline for a wise behaviour.

Keywords: biomedical control; behavioral epidemiology; COVID-19; social distancing; SIR model; flatness-based control; model-free control; robustness

1. Introduction

The social distancing strategies and in particular the severe lockdown measures due to the worldwide COVID-19 pandemic (see, e.g., [1]) have stimulated a huge number of mathematically oriented investigations among which we select control-theoretic publications: See, e.g., [2–35]. Most diverse viewpoints have been developed. Those studies however do not seem to exert any influence on policy-makers (see, e.g., [36] for some explanations). Our aim is to start drawing a roadmap in order to change this state of affairs.

Like many authors in the above–mentioned works, we select the classic SIR compartmental model [37] (see also, e.g., [38–40]). An excellent justification for employing such a simple model has been presented by Sontag [33]: *The social and political use of epidemic models must take into account their degree of realism. Good models do not incorporate all possible effects, but rather focus on the basic mechanisms in their simplest possible fashion. Not only it is difficult to model every detail, but the more details the more the likelihood of making the model sensitive to parameters and assumptions, and the more difficult it is to understand and interpret the model as well as to play what-if scenarios to compare alternative containment policies. It turns out that even simple models help pose important questions about the underlying mechanisms of infection spread and possible means of control of an epidemic.* In addition, the rate of infection and other

fundamental quantities are difficult, if not impossible, to know precisely (see, e.g., [41–43]). This epistemological hindrance to mathematical epidemiology provides further legitimacy for using a parsimonious modeling.

The *transmission rate β*, which corresponds to the social interactions and infection probability per contact, is chosen as the control variable, like in most papers which are quoted above. Thus, our work can be framed in the field of behavioural epidemiology of the infectious disease (see, e.g., [44]).

The SIR model happens then to be (*differentially*) *flat*. This concept [45,46] (see also the books [47–50]) has given rise, as is commonly known, to numerous concrete applications mainly in engineering (see, e.g., [51] for a recent excellent publication about cranes), but also in other domains (see, e.g., [52] in quantum physics). Also of particular interest here is its use [53] for COVID-19 predictions. Take a flat system with a single control variable $u(t)$ and a flat output variable $y(t)$. From a suitable reference trajectory $y^*(t)$, i.e., a suitable time-function, the corresponding open-loop nominal control variable $u^*(t)$ is derived at once from the flatness property. Severe uncertainties, like model mismatch, poorly known initial conditions, external disturbances, ..., prompt us to mimic what has been already done by [18,54,55], i.e., to close the loop via *model-free* control in the sense of [56,57]. Among the numerous remarkable concrete applications of this approach let us cite some recent ones in different domains (see, e.g., [58–62]), and, especially here, mask ventilators for COVID-19 patients [63]. Take another output variable $z(t)$ and its corresponding reference trajectory $z^*(t)$. The feedback loop, which relates $\Delta\beta = \beta - \beta^*$ and the tracking error $\Delta z = z - z^*$, is expressed as an *intelligent Proportional*, or *iP*, controller [56]. This is much easier to implement than traditional PI and PID controllers (see, e.g., [64]) and ensures local stability around z^* with a remarkable level of robustness. Inspired by techniques in [65,66], which were performed in practice for a greenhouse and ramp metering on highways, we close the loop such that the control variable $u = u^* + \Delta u$

- takes only a finite number of numerical values,
- remains constant during some time interval, two weeks here, in our computer simulations.

These features, which are new to the best of our knowledge, imply a limited number of different non-pharmaceutical interventions which moreover are not too severe. They might therefore be socially acceptable. Only low computing capacity is necessary for conducting numerous *in silico* experiments, i.e., computer experiments.

Our paper is organized as follows. The flatness property of the SIR model is shown in Section 2. An open-loop strategy is easily derived in Section 2.2. Section 3 introduces closed-loop control via model-free control. Several computer simulations, which considerably improve [18], are displayed in Section 4. Section 5 is devoted to a discussion of the possible implications of our approach.

2. SIR and Open-Loop Control

2.1. Flatness

The well known SIR model which studies the populations of *susceptible*, whose fraction is denoted as *S*, *infectious*, whose fraction is denoted as *I*, and *recovered* or *removed*, whose fraction is denoted as *R*), reads:

$$\begin{cases} \dot{S} = -\beta IS \\ \dot{I} = \beta IS - \gamma I \\ \dot{R} = \gamma I \end{cases} \tag{1}$$

The transmission rate β and the *recovery/removal rate* γ are positive. Equation (1) yields that $S + I + R$ is constant. We may set

$$S + I + R = 1$$

Straightforward calculations yield:

$$\begin{cases} I = \dfrac{\dot{R}}{\gamma} \\[2ex] S = 1 - R - I = 1 - R - \dfrac{\dot{R}}{\gamma} \\[2ex] \beta = -\dfrac{\dot{S}}{IS} = \dfrac{\gamma\dot{R} + \ddot{R}}{\dot{R}\left(1 - R - \dfrac{\dot{R}}{\gamma}\right)} \end{cases} \tag{2}$$

The system variables I, S and β may be expressed as rational *differential* functions of R, i.e., as rational functions of R and its derivatives up to some finite order. In other words, System (1) is, as already observed [18], flat, and R is a flat output.

Remark 1. *The SEIR (Susceptible-Exposed-Infected-Recovered/Removed) model (see, e.g., [38,39]) is a rather popular extension of the SIR model:*

$$\begin{cases} \dot{S} = -\beta IS \\ \dot{E} = \beta IS - \alpha E \\ \dot{I} = \alpha E - \gamma I \\ \dot{R} = \gamma I \end{cases} \tag{3}$$

where $\alpha > 0$ is an additional parameter. Now

$$S + E + I + R = 1. \tag{4}$$

Equations (3) and (4) show that the SEIR model is flat and that R is again a flat output:

$$\begin{cases} I = \dfrac{\dot{R}}{\gamma} \\[2ex] E = \dfrac{\dot{I} + \gamma I}{\alpha} = \dfrac{\ddot{R} + \gamma\dot{R}}{\gamma\alpha} \\[2ex] S = 1 - R - I - E = 1 - R - \dfrac{\dot{R}}{\gamma} - \dfrac{\ddot{R} + \gamma\dot{R}}{\gamma\alpha} \\[2ex] \beta = -\dfrac{\dot{S}}{IS} \end{cases}$$

2.2. Elementary Formulae for Open-Loop Control

Select the following decreasing exponential reference trajectory, where

- $\lambda > 0$,
- contrarily to [18] we do not start with $R^*(0) = 0$,

$$R^*(t) = \Lambda \exp(-\lambda t) + R^*(\infty) \tag{5}$$

The quantities Λ, $R^*(\infty) = \lim_{t \to +\infty} R^*(t)$ are given below. Formulae (2) and (5) yield

$$I^*(t) = -\dfrac{\Lambda\lambda \exp(-\lambda t)}{\gamma} \tag{6}$$

Formula (6) implies of course that $\Lambda < 0$. The fundamental constraint

$$\lambda < \gamma$$

follows at once from the obvious differential inequality $\dot{I} > -\gamma I$. Moreover

$$S^*(t) = 1 - R^*(\infty) - \Lambda(1 - \frac{\lambda}{\gamma})\exp(-\lambda t) \tag{7}$$

The corresponding open loop control reads

$$\beta^*(t) = \frac{\gamma(\gamma - \lambda)}{(1 - R^*(\infty))\gamma + \Lambda(\lambda - \gamma)\exp(-\lambda t)}$$

Note that $\beta^*(t) > 0$. Thus

$$\beta^*(\infty) = \lim_{t \to +\infty} \beta^*(t) = \frac{\gamma - \lambda}{1 - R(\infty)} \tag{8}$$

The parameter Λ in Equation (5) may be expressed thanks to Equation (6):

$$\Lambda = -\frac{\gamma}{\lambda}I^*(0)$$

Thus

$$R^*(\infty) = R^*(0) - \frac{\gamma}{\lambda}I^*(0)$$

In order to avoid discontinuities at time $t = 0$, set $R^*(0) = R(0)$, $I^*(0) = I(0)$. The following expressions for λ and $R^*(\infty)$ will be used:

$$\Lambda = -\frac{\gamma}{\lambda}I(0)$$

$$R^*(\infty) = R(0) - \frac{\gamma}{\lambda}I(0)$$

$$\beta^*(\infty) = \frac{\lambda(\gamma - \lambda)}{(1 + R(0))\lambda + \gamma I(0)} \tag{9}$$

Introduce the more or less precise quantity β_{accept}: It is the "harshest" social distancing protocols which is "acceptable" in the long run. Equation (9) yields

$$\beta_{\text{accept}} = \frac{\lambda(\gamma - \lambda)}{(1 + R(0))\lambda + \gamma I(0)}$$

and an algebraic equation of degree 2 for determining λ

$$\lambda^2 - \lambda\big((R^*(0) - 1)\beta_{\text{accept}} + \gamma\big) - \gamma I^*(0)\beta_{\text{accept}} = 0 \tag{10}$$

The two roots of Equation (10) are real. The only positive one

$$\frac{(R(0) - 1)\beta_{\text{accept}} + \gamma + \sqrt{[(R(0) - 1)\beta_{\text{accept}} + \gamma]^2 + 4\gamma I(0)\beta_{\text{accept}}}}{2}$$

is the value of λ we are looking for. The corresponding reference trajectory and nominal open-loop control follow at once.

3. Closed-Loop Control

In order to take into account the poor modeling via Equation (1), introduce the *ultra-local* model [56]

$$\frac{d}{dt}\Delta I = \mathcal{F} + \mathfrak{a}\Delta\beta \tag{11}$$

where

- $\Delta I = I - I^*$, $\Delta\beta = \beta - \beta^*$,
- the constant parameter $\mathfrak{a}$, which does not need to be precisely determined, is chosen such that the three terms in Equation (11) are of the same magnitude.
- $\mathcal{F}$ subsumes the poorly known internal structure and the external disturbances.
- An estimate $\mathcal{F}_{est}$ of $\mathcal{F}$ is given [56] by the integral

$$\mathcal{F}_{est} = -\frac{6}{\tau^3} \int_{t-\tau}^{t} ((t - 2\sigma)\Delta I(\sigma) + \mathfrak{a}\sigma(\tau - \sigma)\Delta\beta(\sigma))d\sigma$$

which in practice may be computed via a digital filter.

An *intelligent proportional*, or *iP*, controller [56] reads

$$\Delta\beta = -\frac{\mathcal{F}_{est} + K_P \Delta I}{\mathfrak{a}} \tag{12}$$

where K_P a classic tuning gain and $\mathcal{F}_{est}$ an estimate of $\mathcal{F}$. Combining Equations (11) and (12) yields

$$\frac{d}{dt}\Delta I + K_P \Delta I = \mathcal{F} - \mathcal{F}_{est} \tag{13}$$

If the estimate $\mathcal{F}_{est}$ is "good", i.e., $\mathcal{F}_{est} \approx \mathcal{F}$, then Equation (13) shows that we are led to a pure integrator. Taking $K_P < 0$ yields at once

$$\lim_{t \to +\infty} \Delta I(t) \approx 0$$

Thus local stability around 0 is ensured in spite of mismatches and external disturbances.

4. Computer Simulations

Set in Equation (1) $\gamma = \gamma_{model} = \frac{1}{7}$. The rate $I(t)$ of infected people is assumed to be counted every 2 h. This time lapse, which is of course too short in practice, has been chosen in order to have enough points for our numerical analysis. The iP (12) is employed in all the scenarios below, with $\mathfrak{a} = 0.01$ and $K_P = 15\mathfrak{a}$. Contrarily to [18], the scenarios below do not necessarily start at the beginning of the epidemic.

4.1. Unrealistic Scenarios

A naïve application of Section 2.2 leads to a continuous evolution of the control variable β, i.e., of the social distancing. This is impossible to implement in real life.

4.1.1. Scenario 1

Let us first assume that $I(0)$ and $R(0)$ are perfectly known. This initial time 0 is set after 35 or 45 days of epidemic spreading, where $\beta = 3.6\gamma_{model}$. Thus $I(0)$ after 35 days is less than after 45 days. Figures 1 and 2 display excellent results, where $\beta_{acccept} = 0.95\gamma_{model}$. Note that, even here, closed-loop control is necessary in order to counteract the unavoidable rounding errors.
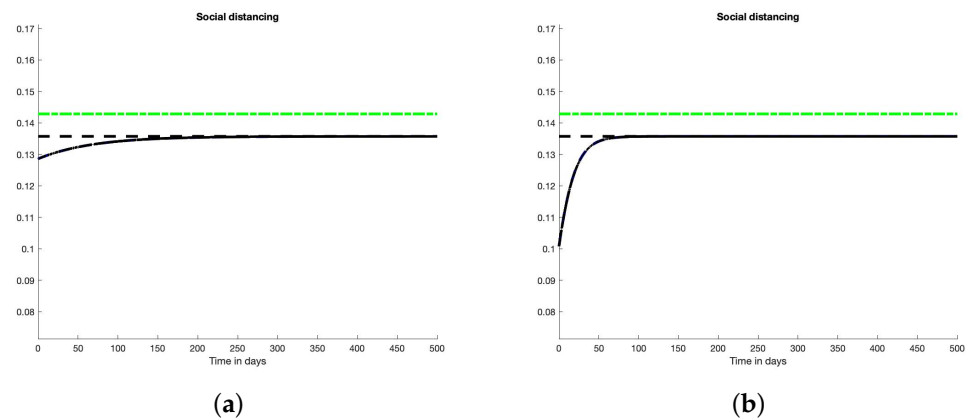
Figure 1. Scenario 1: Open-loop control. (**a**) 35 days later: β, β^* (- -, blue), γ (- ., green) and $\beta_{acceptable}$ (- -, black); (**b**) 45 days later: β, β^* (- -, blue), γ (- ., green) and β_{accept} (- -, black).
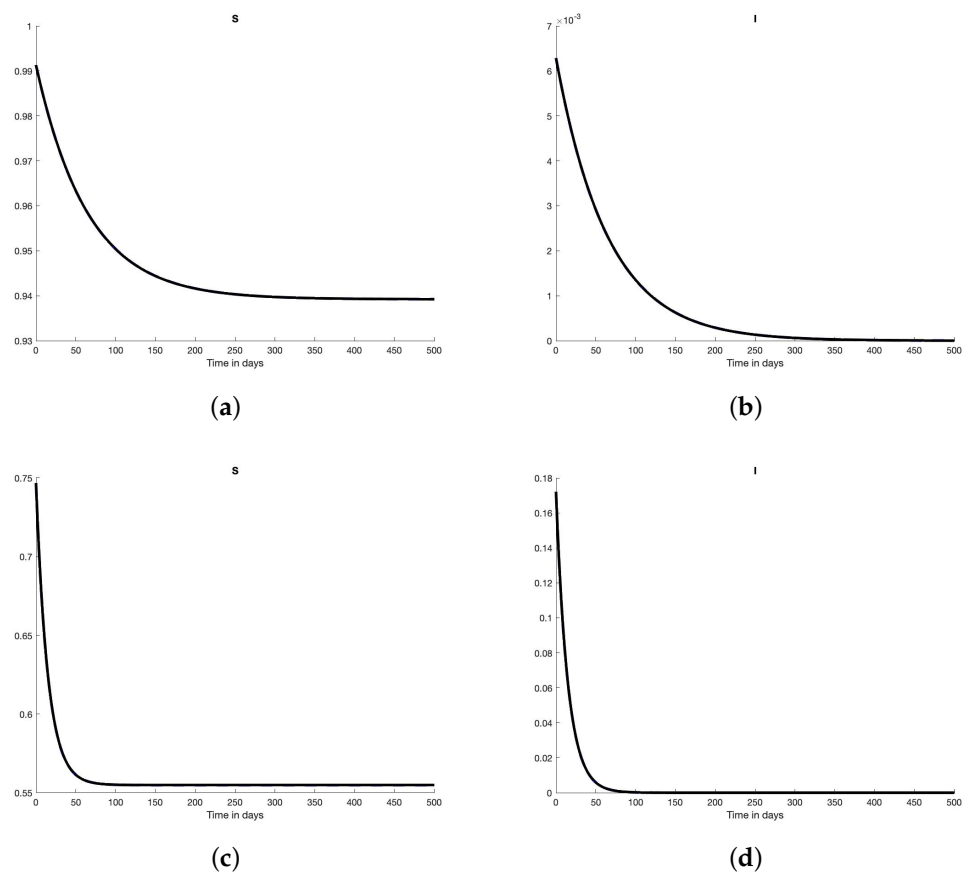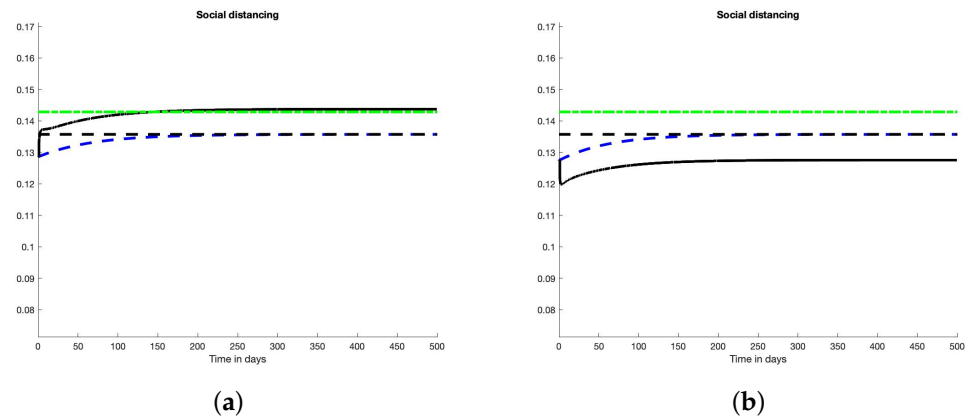

Figure 2. Scenario 1: States. (**a**) 35 days later: S and S^* (- -); (**b**) 35 days later: I and I^* (- -); (**c**) 45 days later: S and S^* (- -); (**d**) 45 days later: I and I^* (- -).
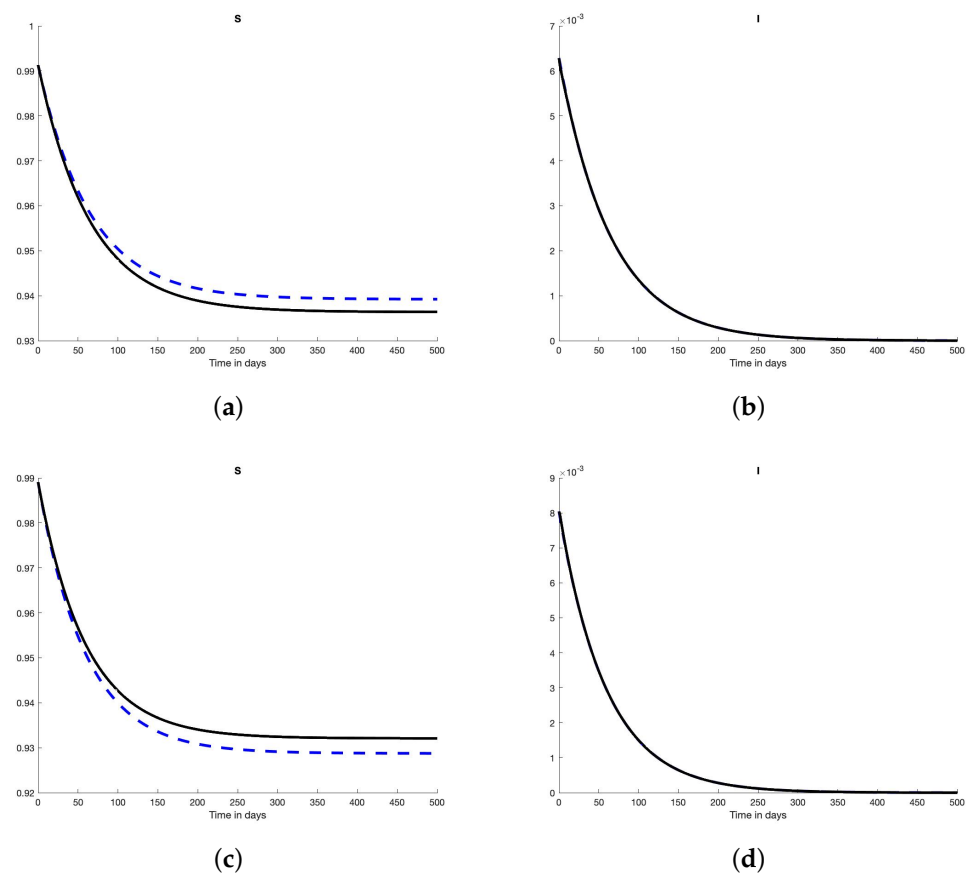
4.1.2. Scenario 2

The initial time is set after 35 days of epidemic spreading. Introduce some mismatches:

- $\gamma_{real} = 1.05 \gamma_{model}$ (Figures 3a and 4a,b),
- $\gamma_{real} = 0.95 \gamma_{model}$ (Figures 3b and 4c,d).

Figure 3. Scenario 2: Control. (**a**) $0.95\gamma_{model}$: β, β^* (- -,blue), γ (- ., green) and $\beta_{acceptable}$ (- -, black); (**b**) $1.05\gamma_{model}$: β, β^* (- -,blue), γ (- ., green) and $\beta_{acceptable}$ (- -, black).

Figure 4. Scenario 2: States. (**a**) $0.95\gamma_{model}$: S and S^* (- -); (**b**) $0.95\gamma_{model}$: I and I^* (- -); (**c**) $1.05\gamma_{model}$: S and S^* (- -); (**d**) $1.05\gamma_{model}$: I and I^* (- -).

It is obvious then that the tracking of I^* yields to deviate from R^* and β^*_{accept}.

4.2. Less Unrealistic Scenarios

Take the same conditions as in Section 4.1.1: no model mismatch, perfectly known initial conditions, the initial time 0 is set after 35 or 45 days of epidemic spreading.

4.2.1. Scenario 3

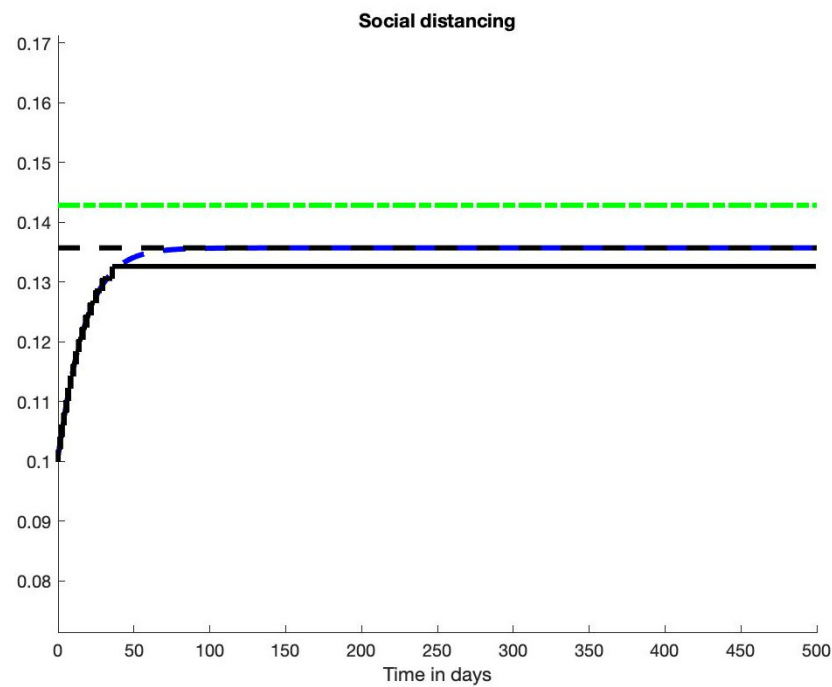Allow only a finite number of numerical values of the control variable β. The control variable β takes 50 uniformly distributed values between $0.5\gamma_{\text{model}}$ and $1.2\gamma_{\text{model}}$. Figures 5 and 6 (35 days) and Figures 7 and 8 (45 days) display excellent results.
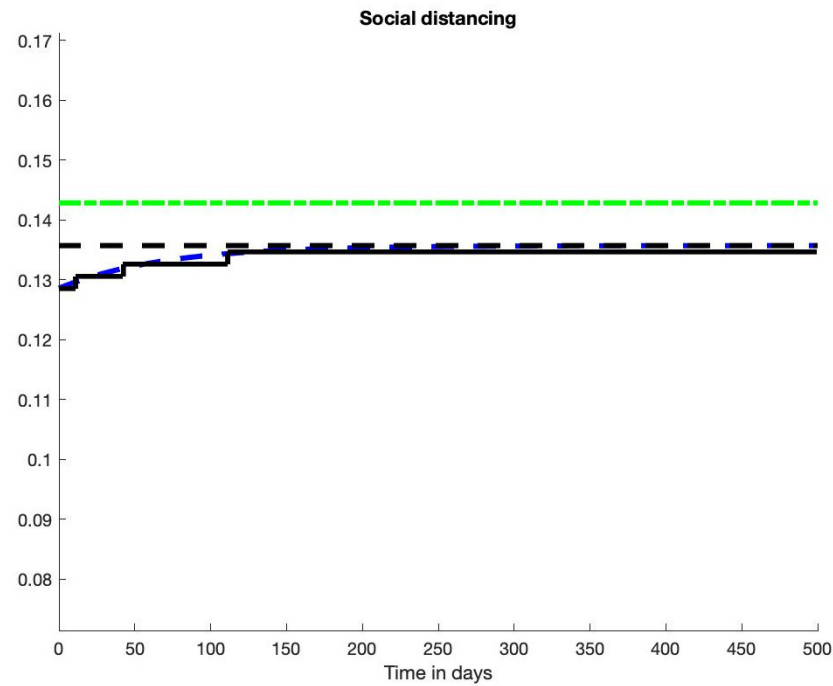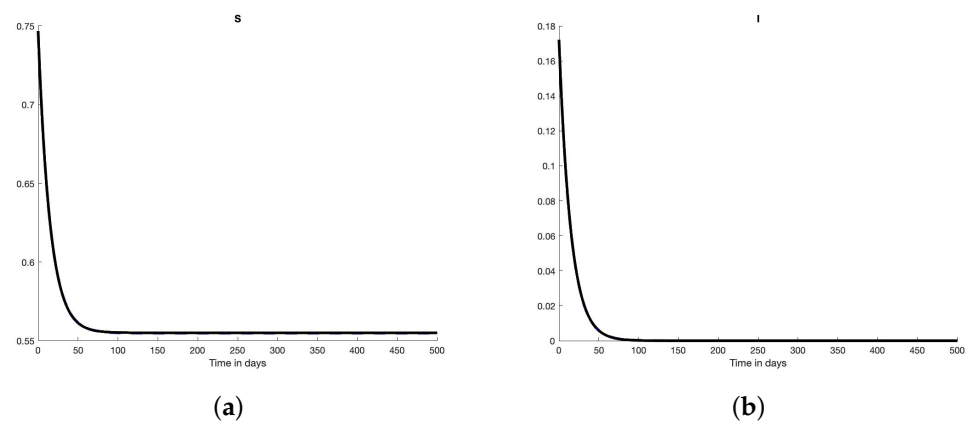

Figure 5. Scenario 3: Control. β, β^* (- -,blue), γ (- ., green) and $\beta_{acceptable}$ (- -, black).
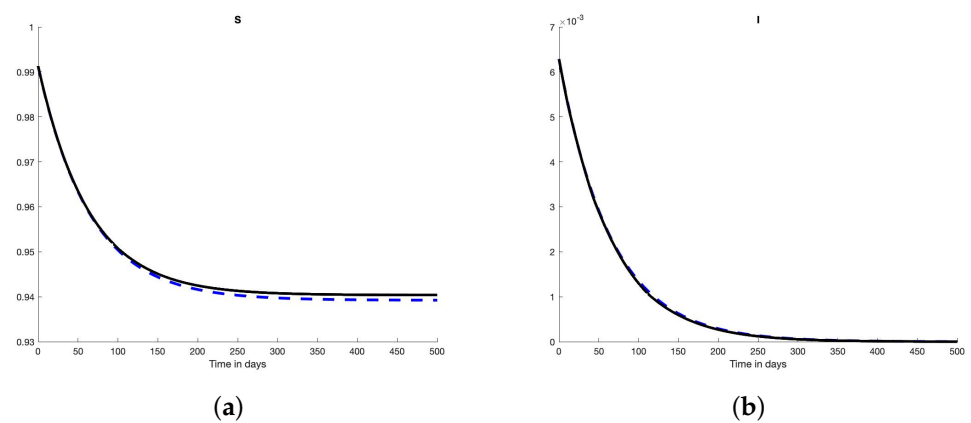
Figure 6. Scenario 3: States. (**a**) S and S^* (- -); (**b**) I and I^* (- -).

Figure 7. Scenario 4: Control. β, β^* (- -,blue), γ (- ., green) and $\beta_{acceptable}$ (- -, black).

| (a) | (b) |

Figure 8. Scenario 4: States. (**a**) S and S^* (- -); (**b**) I and I^* (- -).

4.2.2. Scenario 4

Allow β now to take any value between $0.5\gamma_{\text{model}}$ and $1.2\gamma_{\text{model}}$ but to change only every 14 days. Figures 9 and 10 (35 days) and Figures 11 and 12 (45 days) display rather violent alternations in the social distancing rules. The tracking of I^* remains good.

Figure 9. Scenario 5: Control. β, β^* (- -,blue), γ (- ., green) and $\beta_{acceptable}$ (- -, black).

(**a**)

(**b**)

Figure 10. Scenario 5: States. (**a**) S and S^* (- -); (**b**) I and I^* (- -).

Figure 11. Scenario 5: Control. β, β^* (- -, blue), γ (- ., green) and $\beta_{acceptable}$ (- -, black).

Figure 12. Scenario 5: States. (**a**) *S* and *S** (- -); (**b**) *I* and *I** (- -).

4.3. Scenarios 5–6: A More Realistic Policy

We follow Section 4.2 and combine the conditions on the control variable *β* of Sections 4.2.1 and 4.2.2. Thus *β* takes only a finite number of values and change every 14 days. Correct results are provided in Figures 13 and 14 (35 days) and Figures 15 and 16 (45 days). The tracking of *I** is still excellent.

Figure 13. Scenario 6: Control. *β*, *β** (- -,blue), *γ* (- ., green) and $\beta_{acceptable}$ (- -, black).

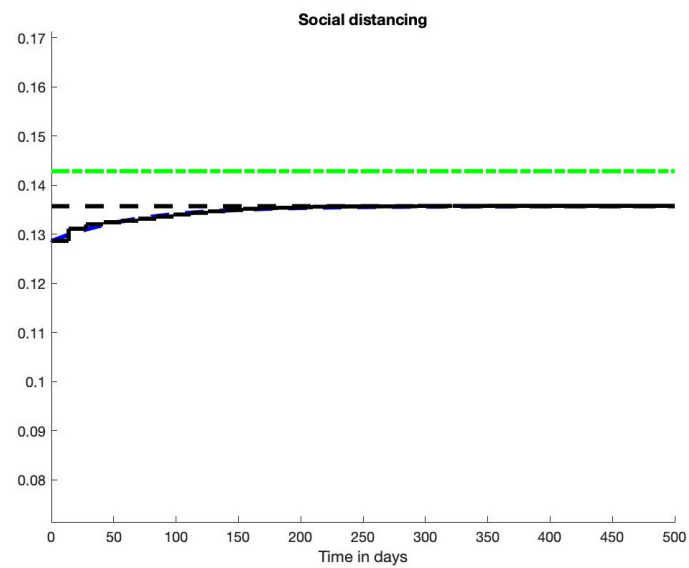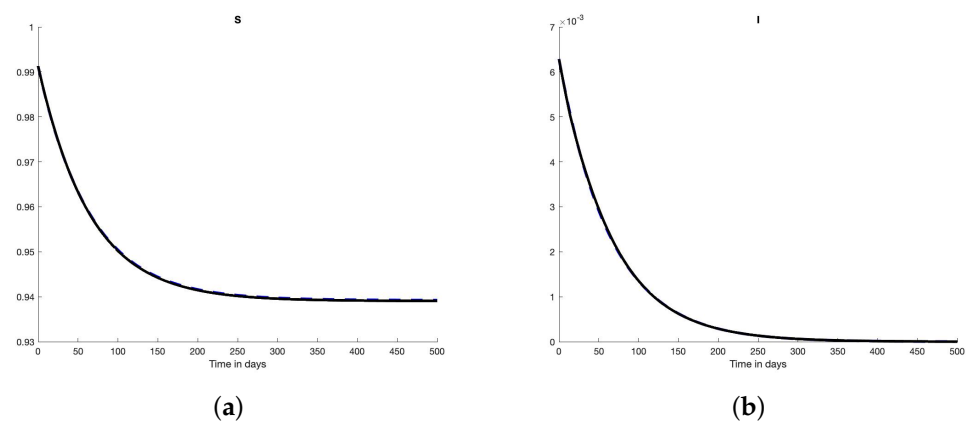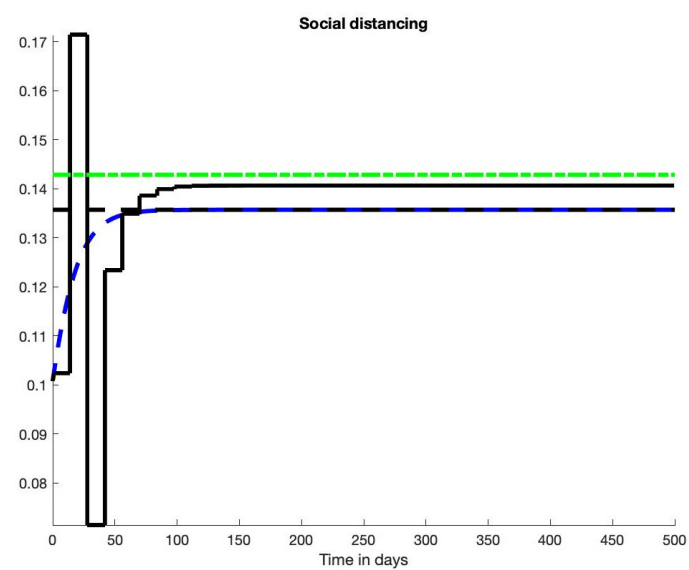**Figure 14.** Scenario 6: States. (**a**) S and S^* (- -); (**b**) I and I^* (- -).

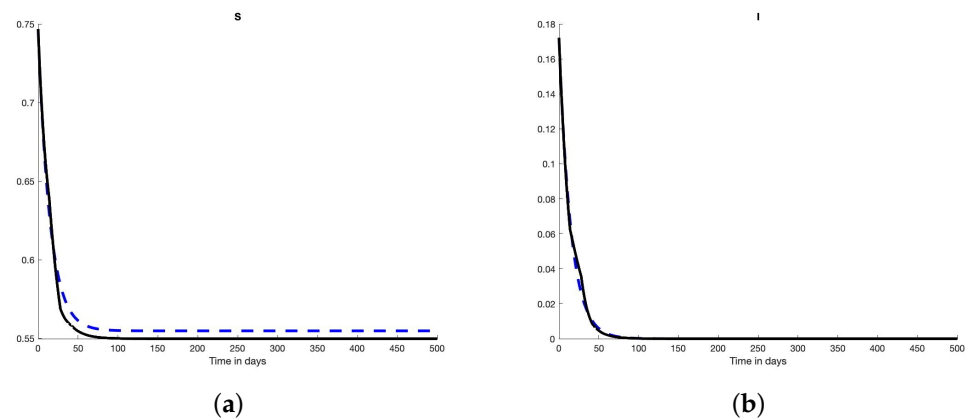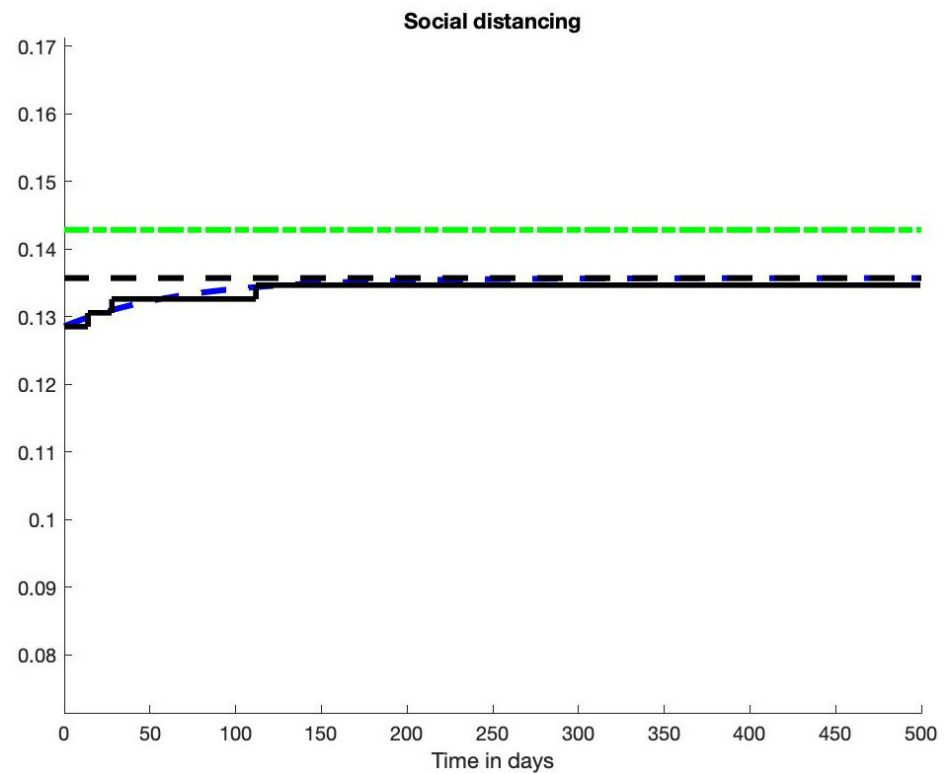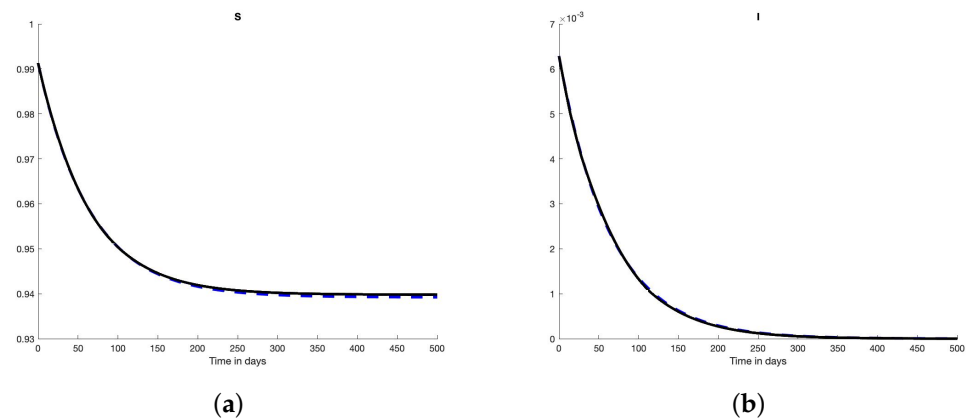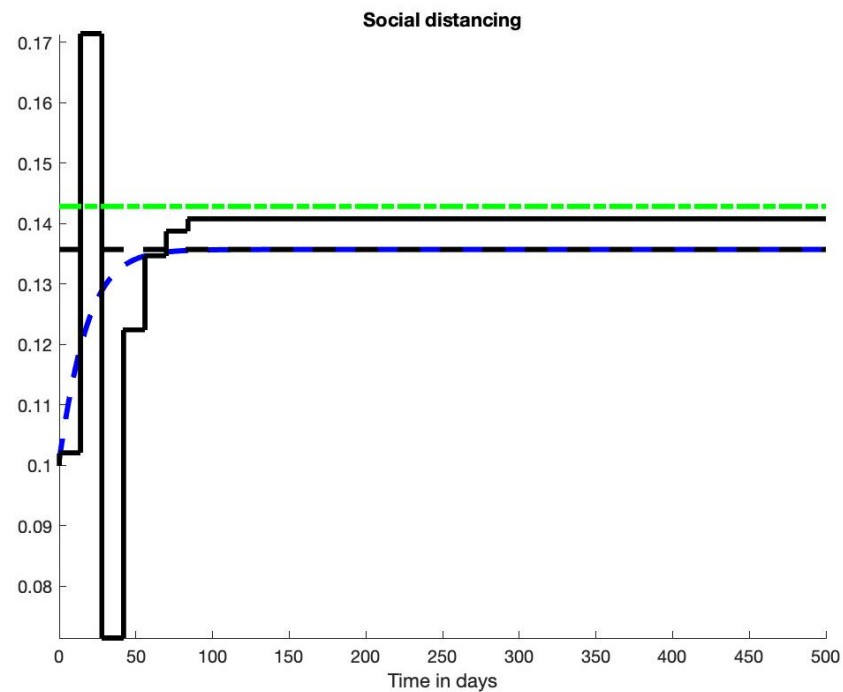**Figure 15.** Scenario 6: Control. β, β^* (- -,blue), γ (- ., green) and $\beta_{acceptable}$ (- -, black).
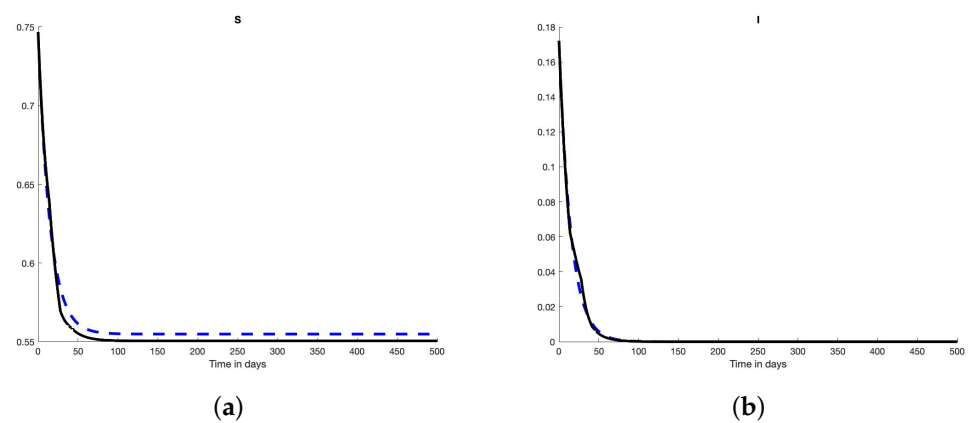

Figure 16. Scenario 6: States. (**a**) S and S^* (- -); (**b**) I and I^* (- -).

5. Conclusions

We have designed a disease mitigation strategy, which is based on recent advances in control synthesis, where

- continuous manipulations of non-pharmaceutical interventions, which are an obstacle to the implementation of the vast majority of theoretical control strategies in epidemiology, even for the remarkably different problem of vaccination awareness campaigns (see [67]), are avoided,
- severe and long lockdowns are replaced by more subtle alternations of more or less strict social distancing measures.

Today empirical control strategies are adopted in practice. However, they are based on the principle of trial and error, which is very risky in epidemic context. Thus, the introduction of more rigorous but realistically constrained approaches might be of interest to policymakers. Another point to be stressed is that our overall results are also robust in presence of uncertainties in key parameters.

Several other questions arise:

- How should one modify the above approach and simulations when vaccinations and variants are taken into account? See, e.g., [68–73] for some preliminary modeling issues.
- Another interrogation is about the interpretation of the numerical values of the control variable β. What is, for instance, the influence of closing nightclubs as done in France and elsewhere? Available estimation techniques would suffer from the poor knowledge of I, and therefore of R and S. This inefficiency includes the techniques employed in [18], where the assumed knowledge of I is unrealistic.

References

1. Adolph, C.; Amano, K.; Bang-Jensen, B.; Fullman, N.; Wilkerson, J. Pandemic politics: Timing state-level social distancing responses to COVID-19. *J. Health Polit. Policy Law* **2021**, *46*, 211–233. [CrossRef] [PubMed]
2. Al-Radhawi, M.A.; Sadeghi, M.; Sontag, E.D. Long-term regulation of prolonged epidemic outbreaks in large populations via adaptive control: A singular perturbation approach. *IEEE Contr. Syst. Lett.* **2022**, *6*, 578–583. [CrossRef]
3. Ames, A.Z.; Molnár, T.G.; Singletary, A.W.; Orosz, G. Safety-critical control of active interventions for COVID-19 mitigation. *IEEE Access* **2020**, *8*, 188454–188474. [CrossRef] [PubMed]
4. Angulo, M.T.; Castaños, F.; Moreno-Morton, R.; Velasco-Hernández, J.X.; Moreno, J.A. A simple criterion to design optimal non-pharmaceutical interventions for mitigating epidemic outbreaks. *J. Roy. Soc. Interface* **2021**, *18*, 20200803. [CrossRef]
5. Berger, T. Feedback control of the COVID-19 pandemic with guaranteed non-exceeding ICU capacity. *Syst. Contr. Lett.* **2022**, *160*, 105111. [CrossRef]
6. Bisiacco, M.; Pillonetto, G. COVID-19 epidemic control using short-term lockdowns for collective gain. *Ann. Rev. Contr.* **2021**, *52*, 573–586. [CrossRef]
7. Bisiacco, M.; Pillonetto, G.; Cobelli, C. Closed-form expressions and nonparametric estimation of COVID-19 infection rate. *Automatica* **2022**, *140*, 110265. [CrossRef]
8. Bliman, P.-A.; Duprez, M. How best can finite-time social distancing reduce epidemic final size? *J. Theoret. Biol.* **2021**, *511*, 110557. [CrossRef]
9. Bliman, P.-A.; Duprez, M.; Privat, Y.; Vauchelet, N. Optimal immunity control and final size minimization by social distancing for the SIR epidemic model. *J. Optim. Theory App.* **2021**, *189*, 408–436. [CrossRef]
10. Bonnans, J.F.; Gianatti, J. Optimal control techniques based on infection age for the study of the COVID-19 epidemic. *Math. Model. Nat. Phenom.* **2020** *15*, 48. [CrossRef]
11. Borri, A.; Palumbo, P.; Papa, F.; Possieri, C. Optimal design of lock-down and reopening policies for early-stage epidemics through SIR-D models *Ann. Rev. Contr.* **2021**, *51*, 511–524. [CrossRef] [PubMed]
12. Charpentier, A.; Elie, R.; Laurière, M.; Tran, V.C. COVID-19 pandemic control: Balancing detection policy and lockdown intervention ICU sustainability. *Math. Model. Nat. Phenom.* **2020**, *15*, 57. [CrossRef]

13. Dias, S.; Queiroz, K.; Araujo, A. Controlling epidemic diseases based only on social distancing level. *J. Contr. Autom. Electr. Syst.* **2022**, *33*, 8–22. [CrossRef]

14. Di Lauro, F.; Kiss, I.Z.; Della Santina, C. Optimal timing of one-shot interventions for epidemic control. *PLoS Comput. Biol.* **2021**, *17*, e1008763. [CrossRef]

15. Di Lauro, F.; Kiss, I.Z.; Della Santina, C. Covid-19 and flattening the curve: A feedback control perspective. *IEEE Contr. Syst. Lett.* **2021**, *5*, 1435–1440. [CrossRef]

16. Efimov, D.; Ushirobira, R. On an interval prediction of COVID-19 development based on a SEIR epidemic model. *Ann. Rev. Contr.* **2021**, *51*, 477–487. [CrossRef]

17. Esterhuizen, W.; Lévine, J.; Streif, S. Epidemic management with admissible and robust invariant sets. *PLoS ONE* **2021**, *16*, e0257598. [CrossRef]

18. Fliess, M.; Join, C.; d'Onofrio, A. Feedback control of social distancing for COVID-19 via elementary formulae. In Proceedings of the 10th Vienna International Conference on Mathematical Modelling, MATHMOD 2022, Vienna, Austria, 27–29 July 2022. Available online: https://hal.archives-ouvertes.fr/hal-03547380/en/ (accessed on 6 April 2022).

19. Gevertz, J.L.; Greene, J.M.; Sanchez-Tapia, C.H.; Sontag, E.D. A novel COVID-19 epidemiological model with explicit susceptible and asymptomatic isolation compartments reveals unexpected consequences of timing social distancing. *J. Theoret. Biol.* **2021**, *510*, 110539. [CrossRef]

20. Greene, J.M.; Sontag, E.D. Minimizing the infected peak utilizing a single lockdown: A technical result regarding equal peak. *MedRxiv* **2021**. [CrossRef]

21. Ianni, A.; Rossi, N. SIR-PID: A proportional-integral-derivative controller for COVID-19 outbreak containment. *Physics* **2021**, *3*, 459–472. [CrossRef]

22. Jing, M.; Yew Ng, K.; Mac Namee, B.; Biglarbeigi, P.; Brisk, R.; Bond, R.; Finlay, D.; McLaughlin, J. COVID-19 modelling by time-varying transmission rate associated with mobility trend of driving via Apple Maps. *J. Biomed. Informat.* **2021**, *122*, 103905. [CrossRef] [PubMed]

23. Köhler, J.; Schwenkel, L.; Koch, A.; Berberich, J.; Pauli, P.; Allgöwer, F. Robust and optimal predictive control of the COVID-19 outbreak. *Ann. Rev. Contr.* **2021**, *51*, 525–539. [CrossRef] [PubMed]

24. McQuade, S.T.; Weightman, R.; Merrill, N.J.; Yadav, A.; Trélat, E.; Allred, S.R.; Piccoli, B. Control of COVID-19 outbreak using an extended SEIR model. *Math. Model. Meth. Appl. Sci.* **2021**, *31*, 2399–2424. [CrossRef]

25. Morato, M.M.; Bastos, S.B.; Cajueiro, D.O.; Normey-Rico, J.E. An optimal predictive control strategy for COVID-19 (SARS-CoV-2) social distancing policies in Brazil. *Ann. Rev. Contr.* **2020**, *50*, 417–431. [CrossRef] [PubMed]

26. Morato, M.M.; Pataro, I.M.L.; da Costa, M.V.A.; Normey-Rico, J.E. A parametrized nonlinear predictive control strategy for relaxing COVID-19 social distancing measures in Brazil. *ISA Trans.* **2020**, *124*, 197–214. [CrossRef]

27. Morgan, A.L.K.; Woolhouse, M.E.J.; Medley, G.F.; van Bunnik, B.A.D. Optimizing time-limited non-pharmaceutical interventions for COVID-19 outbreak control. *Phil. Trans. Roy. Soc. B* **2021**, *376*, 20200282. [CrossRef]

28. Morris, D.H.; Rossine, F.W.; Plotkin, J.B.; Levin, S.A. Optimal, near-optimal, and robust epidemic control. *Communic. Phys.* **2021**, *4*, 78. [CrossRef]

29. O'Sullivan, D.; Gahegan, M.; Exeter, D.J.; Adams, B. Spatially explicit models for exploring COVID-19 lockdown strategies. *Trans. GIS* **2020**, *24*, 967–1000. [CrossRef]

30. Péni, T.; Csutak, B.; Szederkényi, G.; Röst, G. Nonlinear model predictive control with logic constraints for COVID-19 management. *Nonlin. Dyn.* **2020**, *102*, 1965–1986. [CrossRef]

31. Pillonetto, G.; Bisiacco, M.; Palù, G.; Cobelli, C. Tracking the time course of reproduction number and lockdown's effect on human behaviour during SARS-CoV-2 epidemic: Nonparametric estimation. *Sci. Rep.* **2021**, *11*, 9772. [CrossRef]

32. Sadeghi, M.; Greene, J.M.; Sontag, E.D. Universal features of epidemic models under social distancing guidelines. *Ann. Rev. Contr.* **2021**, *51*, 426–440. [CrossRef] [PubMed]

33. Sontag, E.D. An explicit formula for minimizing the infected peak in an SIR epidemic model when using a fixed number of complete lockdowns. *Int. J. Robust Nonlin. Contr.* **2021**. [CrossRef]

34. Stella, L.; Pinel Martínez, A.; Bauso, D.; Colaneri, P. The role of asymptomatic infections in the COVID-19 epidemic via complex networks and stability analysis. *SIAM J. Contr. Optim.* **2022**, S119–S144. [CrossRef]

35. Tsay, C.; Lejarza, F.; Stadtherr, M.A.; Baldea, M. Modeling, state estimation, and optimal control for the US COVID-19 outbreak. *Scientif. Rep.* **2020**, *10*, 10711. [CrossRef] [PubMed]

36. Casella, F. Can the COVID-19 epidemic be controlled on the basis of daily test reports? *IEEE Contr. Syst. Lett.* **2021**, *5*, 1079–1084. [CrossRef]

37. Kermack, W.O.; McKendrick, A.G. A contribution to the mathematical theory of epidemics. *Proc. R. Soc. Lond. Ser. A* **1927**, *115*, 700–721.

38. Brauer, F.; Castillo-Chavez, C. *Mathematical Models in Population Biology and Epidemiology*, 2nd ed.; Springer: New York, NY, USA, 2012.

39. Hethcote, H.W. The mathematics of infectious diseases. *SIAM Rev.* **2020**, *42*, 599–603. [CrossRef]

40. Murray, J.D. *Mathematical Biology I. An Introduction*, 3rd ed; Springer: Berlin/Heidelberg, Germany, 2002.

41. Havers, F.P.; Reed, C.; Lim, T.; Montgomery, J.M.; Klena, J.D.; Hall, A.J.; Thornburg, N.J. Seroprevalence of antibodies to SARS-CoV-2 in 10 sites in the United States, March 23–May 12, 2020. *JAMA Intern. Med.* **2020**, *180*, 1576–1586. [CrossRef]

42. Pérez-Rechel, F.J.; Forbes, K.J.; Strachan, N.J.C. Importance of untested infectious individuals for interventions to suppress COVID-19. *Nat. Sci. Rep.* **2021**, *11*, 20728. [CrossRef]

43. Perkins, T.A.; Cavany, S.A.; Moore, S.M.; Oidtman, R.J.; Lerch, A.; Poterek, M. Estimating unobserved SARS-CoV-2 infections in the United States. *Proc. Natl. Acad. Sci. USA* **2020**, *117*, 22597–22602. [CrossRef]

44. Manfredi, P.; d'Onofrio, A. (Eds.) *Modeling the Interplay Between Human Behavior and the Spread of Infectious Diseases*; Springer: New York, NY, USA, 2013.

45. Fliess, M.; Lévine, J.; Martin, P.; Rouchon, P. Flatness and defect of non-linear systems: Introductory theory and examples. *Int. J. Contr.* **1995**, *61*, 1327–1361. [CrossRef]

46. Fliess, M.; Lévine, J.; Martin, P.; Rouchon, P. A Lie-Bäcklund approach to equivalence and flatness of nonlinear systems. *IEEE Trans. Automat. Contr.* **1999**, *44*, 922–937. [CrossRef]

47. Lévine, J. *Analysis and Control of Nonlinear Systems: A Flatness-Based Approach*; Springer: Berlin/Heidelberg, Germany, 2009.

48. Rigatos, G.G. *Nonlinear Control and Filtering Using Differential Flatness Approaches—Applications to Electromechanical Systems*; Springer: Berlin/Heidelberg, Germany, 2015.

49. Rudolph, J. *Flatness-Based Control: An Introduction*; Shaker Verlag: Düren, Germany, 2021.

50. Sira-Ramírez, H.; Agrawal, S.K. *Differentially Flat Systems*; Marcel Dekker: New York, NY, USA, 2004.

51. Bonnabel, S.; Clayes, X. The industrial control of tower cranes: An operator-in-the-loop approach. *IEEE Contr. Syst. Magaz.* **2020**, *40*, 27–39. [CrossRef]

52. Guéry-Odelin, D.; Ruschhaupt, A.; Kiely, A.; Torrontegui, E.; Martínez-Garaot, S.; Muga, J.G. Shortcuts to adiabaticity: Concepts, methods, and applications. *Rev. Mod. Phys.* **2019**, *91*, 045001. [CrossRef]

53. Hametner, C.; Böhler, L.; Kozek, M.; Bartlechner, J.; Ecker, O.; Du, Z.P.; Kölbl, R.; Bergmann, M.; Bachleitner-Hofmann, T.; Jakubek, S. Intensive care unit occupancy predictions in the COVID-19 pandemic based on age-structured modelling and differential flatness. *Nonlin. Dyn.* **2022**, 1–19. [CrossRef]

54. Fliess, M.; Join, C.; Moussa, K.; Djouadi, S.M.; Alsager, M.W. Toward simple in silico experiments for drugs administration in some cancer treatments. *IFAC PapersOnLine* **2021**, *54*, 245–250. [CrossRef]

55. Villagra, J.; Herrero-Pérez, D. A comparison of control techniques for robust docking maneuvers of an AGV. *IEEE Trans. Contr. Syst. Techno.* **2012**, *20*, 1116–1123. [CrossRef]

56. Fliess, M.; Join, C. Model-free control. *Int. J. Contr.* **2013**, *86*, 2228–2252. [CrossRef]

57. Fliess, M.; Join, C. An alternative to proportional-integral and proportional-integral-derivative regulators: Intelligent proportional-derivative regulators. *Int. J. Robust Nonlin. Contr.* **2021**. [CrossRef]

58. Kuruganti, T.; Olama, M.; Dong, J.; Xue, Y.; Winstead, C.; Nutaro, J.; Djouadi, S.; Bai, L.; Augenbroe, G.; Hill, J. *Dynamic Building Load Control to Facilitate High Penetration of Solar Photovoltaic Generation: Final Technical Report (No. ORNL/TM-2021/2112)*; Oak Ridge National Lab: Oak Ridge, TN, USA, 2021.

59. Lv, M.; Gao, S.; Wei, Y.; Zhang, D.; Qi, H.; Wei, Y. Model-free parallel predictive torque control based on ultra-local model of permanent magnet synchronous machine. *Actuators* **2022**, *11*, 31. [CrossRef]

60. Michel, L; Neunaber, I; Mishra, R.; Braud, C.; Plestan, F.; Barbot, J.-P.; Boucher, X.; Join, C.; Fliess M. Model-free control of the dynamic lift of a wind turbine blade section: experimental results. *J. Physics Conf. Series* **2022**, *2265*, 032068. [CrossRef]

61. Sancak, C.; Yamac, F.; Itik, M.; Alici, G. Force control of electro-active polymer actuators using model-free intelligent control. *J. Intel. Mater. Syst. Struct.* **2021**, *32*, 2054–2065. [CrossRef]

62. Wang, Z.; Cosio, A.; Wang, J. Implementation resource allocation for collision-avoidance assistance systems considering driver capabilities. *IEEE Trans. Intel. Transport. Syst.* **2021**. [CrossRef]

63. Truong, C.T.; Huynh, K.H.; Duong, V.T.; Nguyen, H.H.; Pham, L.A.; Nguyen, T.T. Model-Free Vol. Press. Cycled Control Autom. Bag Valve Mask Vent. *AIMS Bioengin.* **2021**, *8*, 192–207. [CrossRef]

64. Åström, K.J.; Murray R.M. *Feedback Systems—An Introduction for Scientists and Engineers*; Princeton University Press: Princeton, NJ, USA, 2008.

65. Lafont, F.; Balmat, J.-F.; Pessel, N.; Fliess, M. A model-free control strategy for an experimental greenhouse with an application to fault accommodation. *Comput. Electron. Agricult.* **2015**, *110*, 139–149. [CrossRef]

66. Join, C.; Abouaïssa, H.; Fliess, M. Ramp metering: Modeling, simulation and control issues. In *Advances in Distributed Parameter Systems*; Auriol, J., Deutscher, J., Mazanti, G., Valmorbid, G., Eds.; Springer: Cham, Switzerland, 2022; pp. 227–242.

67. Della Marca, R.; d'Onofrio, A. Volatile opinions and optimal control of vaccine awareness campaigns: Chaotic behaviour of the forward-backward sweep algorithm vs. heuristic direct optimization. *Commun. Nonlin. Sci. Numer. Simulat.* **2021**, *98*, 105768. [CrossRef]

68. Arruda, E.F.; Das, S.S.; Dias, C.M.; Pastore, D.H. Modelling and optimal control of multi strain epidemics, with application to COVID-19. *PLoS ONE* **2021** *16*, e0257512. [CrossRef]

69. Kopfová, J.; Nábělková, P.; Rachinskii, D.; Rouf, S.C. Dynamics of SIR model with vaccination and heterogeneous behavioral response of individuals modeled by the Preisach operator. *J. Math. Bio.* **2021**, *83*, 11. [CrossRef]

70. Laguzet, L.; Turinici, G. Global optimal vaccination in the SIR model: Properties of the value function and application to cost-effectiveness analysis. *Math. Biosci.* **2015**, *263*, 180–197. [CrossRef]

71. Moore, S.; Hill, E.M.; Tildesley, M.J.; Dyson, L.; Keeling, M.J. Vaccination and non-pharmaceutical interventions for COVID-19: A mathematical modelling study. *Lancet Infect. Dis.* **2021**, *21*, 793–802. [CrossRef]

72. d'Onofrio, A.; Manfredi, P.; Salinelli, E. Vaccinating behaviour, information, and the dynamics of SIR vaccine preventable diseases. *Theoret. Populat. Bio.* **2007**, *71*, 301–317. [CrossRef] [PubMed]

73. Ramos, A.M.; Vela-Pérez, M.; Ferrández, M.R.; Kubik, A.B.; Ivorra, B. Modeling the impact of SARS-CoV-2 variants and vaccines on the spread of COVID-19. *Commun. Nonlin. Sci. Numer. Simulat.* **2021**, *102*, 105937. [CrossRef] [PubMed]